program. The authors would like to thank Dansen Brown, U.S. Air Force Research Laboratory/VASS, for his invaluable assistance in data analysis. Also, the authors gratefully acknowledge the assistance and expertise of Larry Simmons, the Structural Dynamics and Acoustics Branch facility technician.

References

[1]Blevins, R. D., Holehouse, I., and Wentz, K. R., "Thermoacoustic Loads and Fatigue of Hypersonic Vehicle Skin Panels," *Journal of Aircraft*, Vol. 30, No. 6, 1993, pp. 971–978.

[2]Vaicaitis, R., "Nonlinear Response and Sonic Fatigue of National Aerospace Plane Surface Panels," *Journal of Aircraft*, Vol. 31, No. 1, 1994, pp. 10–18.

[3]Chen, R. R., Mei, C., and Wolfe, H. F., "Comparison of Finite Element Nonlinear Beam Random Response with Experimental Results," *Journal of Sound and Vibration*, Vol. 195, No. 5, 1996, pp. 719–737.

[4]Ibrahim, R. A., "Nonlinear Random Vibration: Experimental Results," *Applied Mechanics Review*, Vol. 44, No. 10, 1991, pp. 423–446.

[5]Wolfe, H. F., Camden, M. P., Wentz, K. R., and Simmons, L. W., "Determining the Peak Probability Distribution Function of the Nonlinear Random Response of a Clamped Plate," *Proceedings of the Second International Conference on Non-Linear Problems in Aviation and Aerospace*, Vol. 2, European Conference Publ., Cambridge, England, U.K., 1999, pp.787–796.

[6]Koenig, K., Gunther, M., and Grahlmann, U., "Some Remarks on the Acoustic Fatigue of Aluminum Structures with either Integrally Milled or Riveted Edge Reinforcements," *Aerospace Science and Technology*, Vol. 2, No. 1, 1998, pp. 27–36.

[7]Ng, C. F., "Nonlinear and Snap-Through Responses of Curved Panels to Intense Acoustic Excitation," *Journal of Aircraft*, Vol. 26, No. 3, 1989, pp. 281–288.

[8]Ng, C. F., and Clevenson, S. A., "High Intensity Acoustic Tests of a Thermally Stressed Plate," *Journal of Aircraft*, Vol. 28, No. 4, 1991, pp. 275–281.

[9]Wolfe, H. F., Shroyer, C. A., Brown, D. L., and Simmons L. W., "An Experimental Investigation of Nonlinear Behavior of Beams and Plates Excited to High Levels of Dynamic Responses," U.S. Air Force Wright Research and Development Center, WL-TR-96-3057 1995 WL/FIBG, Wright–Patterson AFB, OH, Oct. 1996.

[10]Istenes, R. R., Rizzi, S. A., and Wolfe, H. F., "Experimental Nonlinear Random Vibration Results of Thermally Buckled Composite Panels," *Proceedings of the 36th Structures, Structural Dynamics, and Materials Conference*, AIAA, Washington, DC, 1995, pp. 1559–1568.

[11]Wolfe, H. F., Camden, M. P., Byrd, L. W., Paul, D. B., and Simmons, L. W., "Failure Criteria Development for Dynamic High-Cycle Fatigue of Ceramic Matrix Composites," *Journal of Aircraft*, Vol. 37, No. 2, 2000, pp. 319–324.

[12]Wolfe, H. F., Camden, L. W., Paul, D. B., and Simmons, L. W., "Sigma Limiting Effects on the Response of a Ceramic Matrix Beam," AIAA Paper 99-1456, 1999.

[13]Randall, R. B., *Frequency Analysis*, K. Larsen and Søn A/S, Glostrup, Denmark, 1987.

[14]Schudt, J. A., "The Response of Nonlinear Systems to Random Excitation," M.S. Thesis, Dept. of Engineering Mechanics, Ohio State Univ., Columbus, OH, 1991.

[15]Mei, C., Dhainaut, J. M., Duan, B., Spottswood, S. M., and Wolfe, H. F., "Nonlinear Random Response of Composite Panels in an Elevated Thermal Environment," U.S. Air Force Research Lab., AFRL-VA-WP-TR-2000-3049, Wright–Patterson AFB, OH, Oct. 2000.

[16]Anzai, H., "Algorithm of the Rainflow Method," *Proceedings of the International Symposium on Fatigue Damage Measurement and Evaluation under Complex Loading. The Rainflow Method in Fatique—The Tatsuo Endo Memorial Volume*, Fukuoka, Japan, 1991, pp. 11–20.

[17]Bannantine, J. A., Comer, J. J., and Handrock J. L., *Fundamentals of Metal Fatigue Analysis,* Prentice–Hall, Upper Saddle River, NJ, 1990, pp. 193–196.

[18]Lee, J., "Displacement and Strain Statistics of Thermally Buckled Plates," *Journal of Aircraft*, Vol. 38, No. 1, 2001, pp. 104–110.

[19]Steinwolf, A., and White, R. G., "Probability Density Functions of Acoustically Induced Strains in Experiments with Composite Plates," *AIAA Journal*, Vol. 35, No. 12, 1997, pp. 1853–1861.

A. N. Palazotto
Associate Editor

Stability of Spring-Hinged Cantilever Column Under Combined Concentrated and Distributed Loads

G. Venkateswara Rao* and K. Kanaka Raju†
Vikram Sarabhai Space Center, Trivandrum 695 022, India

Nomenclature

a, b	=	undetermined coefficients in Eq. (6)
a_1–a_6	=	functions defined in Eq. (8)
E	=	Young's modulus
I	=	area moment of inertia
k	=	stiffness of the rotational spring
L	=	length of the column
P	=	end-concentrated axial load
P_{cr}	=	critical P
q	=	uniformly distributed axial load
q_{cr}	=	critical q
W	=	lateral displacement distribution
w	=	nondimensional lateral displacement, W/L
α	=	$\lambda_q/\lambda_{q\,cr}$
α_1–α_3	=	undetermined coefficients in Eq. (2)
β	=	$\lambda_P/\lambda_{p\,cr}$
γ	=	rotational spring stiffness parameter, kL/EI
λ_p	=	concentrated axial load parameter, PL^2/EI
λ_q	=	uniformly distributed axial load parameter, qL^3/EI
$\lambda_{p\,cr}$	=	critical λ_p
$\lambda_{q\,cr}$	=	critical λ_q
ξ	=	nondimensional axial coordinate x, x/L
$'$	=	differentiation with respect to ξ

Introduction

THE upper stage of solid motor rockets and missiles is a highly optimized structure required to be designed to achieve higher payload capability. The fore end of this stage is connected to the payload through a payload adaptor, and the aft end is connected to a relatively stiffer stage through interstage structure that is flexible in rotation. In service condition, the rockets and missiles are subjected to very high axial acceleration. Because of this and the mass of the payload and payload adaptor, the fore end of the upper stage is subjected to a high axial compressive concentrated load. The upper stage is also subjected to a uniformly distributed axial compressive load due to its own inertia. As such, the upper stage can be idealized as a uniform cantilever column simultaneously subjected to an axial compressive concentrated load at the free end and a uniformly distributed axial compressive load along the length of the column, the two loads being mutually independent and acting simultaneously. The aft end of the column, where rotation is allowed, can be modeled as a spring-hinged end because of the rotational flexibility of the interstage structure with the lateral displacement constrained. Thus, the analytical model turns out to be a three-parameter problem, and it is often necessary to obtain the stability behavior of such columns to assess their structural integrity.

Even though the versatile finite element method[1] (FEM) can be effectively used to solve this problem, it becomes laborious and time consuming because of the parametric study involved with three parameters. Hence, development of an accurate closed-form solution

Received 4 April 2001; revision received 14 September 2001; accepted for publication 9 May 2002.

*Scientist/Engineer, Structural Engineering Group; gv_rao@vssc.org.
†Scientist/Engineer, Structural Engineering Group.

is very attractive and is attempted in the present Note, using the technique followed by Elishakoff,[2] to simulate the rotational elastic restraint at the spring-hinged end. The Rayleigh–Ritz method is employed to obtain the solution. The method is validated independently for a concentrated compressive load at the free end and for a uniform axial compressive load along the length of the column with rotational elastic restraint at the other end, by comparison of the present results with those obtained by the use of the FEM. The effect of the combined loads with elastic restraint is studied, and the numerical results are presented in a user-friendly form.

Energy Formulation

Consider a spring-hinged cantilever column subjected to a compressive concentrated load P at the free end and a uniform compressive load q per unit length acting along the length of the column, as shown in Fig. 1. To obtain buckling critical values of P and q, when applied in combination, the following is proposed.

The total potential energy of the column is given by

$$\Pi = \frac{EI}{2}\int_0^L W''^2\,\mathrm{d}x + \frac{1}{2}kW'^2\bigg|_{x=0} - \frac{P}{2}\int_0^L W'^2\,\mathrm{d}x - \frac{q}{2}\int_0^L (1-x)W'^2\,\mathrm{d}x \tag{1}$$

Following Elishakoff,[2] the lateral displacement distribution is assumed as

$$w = \alpha_1\xi + \alpha_2\xi^2 + \alpha_3\xi^3 \tag{2}$$

Equation (2) satisfies the boundary condition

$$w(o) = 0 \tag{3}$$

The spring-hinged condition is

$$(EI/L)w''(o) = kw'(o) \tag{4}$$

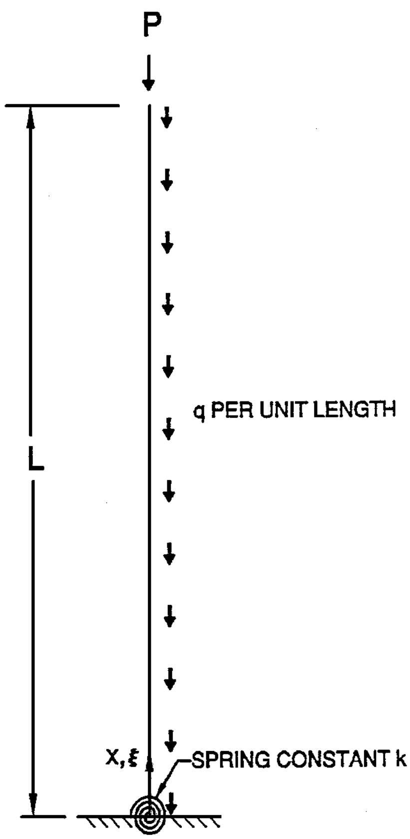

Fig. 1 Spring-hinged cantilever column subjected to combined end-concentrated and uniformly distributed axial compressive loads.

From Eqs. (2) and (4), we get

$$\alpha_1 = (2/\gamma)\alpha_2 \tag{5}$$

Hence, the admissible displacement distribution w for this problem becomes

$$w = a[(2/\gamma)\xi + \xi^2] + b\xi^3 \tag{6}$$

Substituting Eq. (6) in Eq. (1), taking variation with respect to a and b, equating them to zero and eliminating a and b (which is a standard Rayleigh–Ritz procedure and, hence, the detailed algebra is not given here), we get the final equation governing λ_p and λ_q as

$$a_1\lambda_p^2 - a_2\lambda_p + a_3\lambda_q^2 - a_4\lambda_q + a_5\lambda_p\lambda_q + a_6 = 0 \tag{7}$$

where

$$a_1 = 3/5 + 24/5\gamma + 64/5\gamma^2$$

$$a_2 = 104/5 + 624/5\gamma + 192/\gamma^2$$

$$a_3 = 1/25 + 2/5\gamma + 7/5\gamma^2$$

$$a_4 = 32/5 + 224/5\gamma + 96/\gamma^2$$

$$a_5 = 2/5 + 18/5\gamma + 56/5\gamma^2$$

$$a_6 = 48 + 192/\gamma \tag{8}$$

For a given γ, Eq. (7) can be solved to obtain $\lambda_{p\,\mathrm{cr}}$ if $\lambda_q = 0$ ($q = 0$) or, if $\lambda_p = 0$ ($P = 0$), then $\lambda_{q\,\mathrm{cr}}$ can be obtained. If both mutually independent P and q are present, the equation for a given γ can be solved for λ_p by assuming for λ_q ($\lambda_q = \alpha\lambda_{q\,\mathrm{cr}}$, $0 < \alpha < 1$), a value that is a fraction of $\lambda_{q\,\mathrm{cr}}$.

Numerical Results and Discussion

Figure 1 shows a uniform spring-hinged cantilever column subjected to a combined axial end load and an axial uniformly distributed load q per unit length. Based on the formulation presented in the preceding section, the combination of P and q at which the column buckles is evaluated for various rotational spring stiffnesses.

Because the admissible functions for use in the Rayleigh–Ritz method are derived following Elishakoff,[2] it is necessary to validate the formulation by comparing the present results with published values that are obtained by another method. This is done separately for an axial end load and axial uniformly distributed load for different rotational spring constants k.

Table 1 gives the critical load parameters $\lambda_{p\,\mathrm{cr}}$ and $\lambda_{q\,\mathrm{cr}}$ obtained independently by the present formulation for several values of the rotational spring stiffness parameter γ. A finite element solution with 16 equal length finite elements, which gives an accurate result up to four significant figures, is obtained for the stability problem of spring-hinged cantilever columns subjected to an axial end load and an axial uniformly distributed load independently for several values of γ. It is seen from Table 1 that the present results agree

Table 1 Critical load parameter $\lambda_{p\,\mathrm{cr}}$ and $\lambda_{q\,\mathrm{cr}}$ values for a spring-hinged cantilever column subjected to independent loads

	Tip concentrated load		Uniform distributed load	
γ	Present study	FEM	Present study	FEM
1	0.7405	0.7402	1.665	1.654
10	2.054	2.043	5.957	5.918
100	2.437	2.421	7.657	7.608
500	2.476	2.459	7.842	7.793
1,000	2.481	2.464	7.865	7.816
10,000	2.485	2.469	7.887	7.840
10^{11} ($\to \infty$)	2.486	2.469	7.890	7.840

Table 2 Critical combination of the load parameters λ_p and λ_q of a spring-hinged cantilever column

γ	$\lambda_{p\,\mathrm{cr}}$	$\lambda_{q\,\mathrm{cr}}$	$\alpha(\lambda_q/\lambda_{q\,\mathrm{cr}})$	λ_p	$\beta(\lambda_p/\lambda_{p\,\mathrm{cr}})$	$\alpha+\beta$
1.0	0.7405	1.665	0.2	0.5942	0.8025	1.002
1.0	0.7405	1.665	0.4	0.4471	0.6038	1.004
1.0	0.7405	1.665	0.6	0.2990	0.4038	1.004
1.0	0.7405	1.665	0.8	0.1500	0.2025	1.002
10	2.054	5.957	0.2	1.655	0.8058	1.006
10	2.054	5.957	0.4	1.250	0.6087	1.009
10	2.054	5.957	0.6	0.8394	0.4087	1.009
10	2.054	5.957	0.8	0.4227	0.2058	1.006
100	2.437	7.657	0.2	1.9640	0.8060	1.006
100	2.437	7.657	0.4	1.4840	0.6090	1.009
100	2.437	7.657	0.6	0.9966	0.4090	1.009
100	2.437	7.657	0.8	0.5020	0.2060	1.006

very well with those obtained from the FEM for all values of the rotational spring stiffness parameter γ varying from 1 to 10^{11} ($\rightarrow\infty$), the maximum error being around 0.7% for the value of $\gamma = 10^{11}$. Also note that the stability parameters obtained by the FEM are in excellent agreement with those given by Timoshenko and Gere.[3]

For the combined loading, the combination values of λ_p and λ_q for which the spring-hinged column buckles are given in Table 2, for $\gamma = 1$, 10, and 100. Note that, for the combined loading, the sum of $\lambda_p/\lambda_{p\,\mathrm{cr}}$ and $\lambda_q/\lambda_{q\,\mathrm{cr}}$ is almost equal to 1.0, with the nonzero term being in the fourth significant figure. The authors have verified this for all of the values of γ considered in Table 1. It is believed that this small difference from unity in the fourth significant figure is due to the numerical approximation involved in the present computations. Hence, we can generalize this observation as follows.

Irrespective of the rotational spring stiffness, for a spring-hinged cantilever column subjected to combined axial concentrated end load and uniformly distributed load, we can take

$$\lambda_p/\lambda_{p\,\mathrm{cr}} + \lambda_q/\lambda_{q\,\mathrm{cr}} = 1 \tag{9}$$

effectively for design purposes. Equation (9) is valid for any mutually independent and simultaneously acting axial compressive concentrated load and uniformaly distributed axial compressive load.

Conclusions

The stability behavior of a spring-hinged cantilever column subjected to mutually independent and simultaneously acting end-compressive and uniformly distributed axial loads is studied in this Note by use of the Rayleigh–Ritz method. The novelty of this study is choosing proper admissible functions to satisfy the spring-hinged boundary condition. Closed-form expressions are obtained for the combination of loads for which the column buckles. The method is validated by comparing the present results with those obtained by the FEM for the cases of independent loads. Finally, a simple, elegant design formula for the combined loading is given based on the numerical results obtained. It is expected that it will be useful for aerospace engineers in particular, and structural engineers, in general.

References

[1]Zienkiewicz, O. C., *The Finite Element Method*, McGraw–Hill Ltd., London, 1977.

[2]Elishakoff, I., "Apparently First Closed-Form Solution for Frequency of Beam with Rotational Spring," *AIAA Journal*, Vol. 39, No. 1, 2001, pp. 183–186.

[3]Timoshenko, S. P., and Gere, J. M., *Theory of Elastic Stability*, McGraw–Hill, New York, 1961, pp. 89–103.

A. M. Waas
Associate Editor

Vortical Substructures in the Shear Layers Forming Leading-Edge Vortices

Anthony M. Mitchell*
U.S. Air Force Academy,
Colorado Springs, Colorado 80840-6222
and
Pascal Molton†
ONERA, 92190 Meudon, France

Introduction

SUBSTANTIAL theoretical, experimental, and computational research has focused on the characteristics of leading-edge vortices and vortex breakdown.[1–8] However, limited efforts have sought to understand the separating shear layers that roll up to form the leading-edge vortices. Various researchers have observed discrete vortical substructures in the shear layers, and the resulting data have taken on two contrasting descriptions: temporal substructures (rotating around the leading-edge vortex)[9–11] and spatially stationary substructures (spatially fixed around the periphery of the leading-edge vortex).[12–19] Additionally, many of these researchers have hypothesized about the type of instability that results in the formation of the vortical substructures. None of these hypotheses has been universally accepted or proven. The most popular hypothesis[9,11,13,14,17,18] proposes that the substructures develop in a manner similar to the Kelvin–Helmholtz[20] instability or that of a two-dimensional shear-layer instability described by Ho and Huerre.[21] Another hypothesis suggests that the substructures originate from transversal perturbations along the leading edge of the wing induced by the interaction between the separating shear layer and the secondary vortices.[10,19] Washburn and Visser[16] suggested the substructures are generated by nonviscous instabilities in the shear layer and that their formation is governed by transverse flow of the leading-edge vortices. Yet another hypothesis postulates that a longitudinal instability associated with the curvature of the separating shear layer is at the origin of the substructures.[17] Some experimentally based hypotheses indicate that the instabilities are generated by the presence of small-amplitude surface waves in the water tunnel[10] or are associated with vibrations in a wind tunnel.[14]

Recent advances in nonintrusive experimental measurement techniques have enabled more detailed analysis of the vortical flowfield and the separating shear layers forming the leading-edge vortices around a delta wing. Three-dimensional laser Doppler velocimetry (LDV) flowfield measurements were acquired in ONERA's 1.4×1.8 m subsonic wind tunnel around a sharp-edged delta wing model.[22–24] These novel results provide new insight into the phenomenon through precisely measured details of the characteristics and path of the vortical substructures around the leading-edge vortex core.

Model and Wind Tunnel

The delta wing model has a 70-deg sweep angle and root chord c of 950 mm. It has a wingspan of 691.5 mm at its trailing edge, is

Presented as Paper 2001-2424 at the 19th Applied Aerodynamics Conference, Anaheim, CA, 11–14 June 2001; received 21 June 2001; revision received 18 April 2002; accepted for publication 18 April 2002.

*Major, U.S. Air Force, and Assistant Professor, Department of Aeronautics, 2354 Fairchild Drive, Suite 6H39C. Senior Member AIAA.

†Research Engineer, Fundamental and Experimental Aerodynamics Department, 8 rue des Vertugadins.